RECENT RESULTS FROM CCFM EVOLUTION*

H. Jung

Experimental High Energy Physics
Department of Physics, Lund University
SE-22100 Lund, Sweden

Recent developments of the small x CCFM evolution are described, including improvements of the splitting function. The resulting unintegrated gluon densities are used for predictions of hadronic final state measurements like jet production at HERA and heavy quark production at the Tevatron.

PACS numbers: 12.38.Bx, 12.38.Cy

This paper is dedicated to the memory of Jan Kwieciński, who passed away so early.

1. The problem with collinear factorization

Inclusive cross section measurements [1,2], but also many hadronic final state cross sections [3–5] are in general well described in QCD. The cross sections are factorized into integrated parton density functions (PDFs) which are evolved from a starting scale μ_0 to the factorization scale μ_f using the DGLAP [6–9] evolution equations and convoluted with the process dependent coefficient functions (matrix elements). This approach is often called collinear factorization.

However, regions in phase space exist where the above mentioned approach using coefficient functions evaluated at fixed order in the strong coupling constant, α_s, is not sufficient to describe the measured cross sections. Such measurements are *e.g.* forward jet production and the azimuthal decorrelation of jets at HERA, but also heavy quark production at the Tevatron.

Processes sensitive to hard multi-parton emissions are generally not covered fully in DGLAP. The BFKL [10–12] approach, also called the k_t-factorization [13, 14] or the semi-hard approach [15, 16], is assumed to be better suited for such a scenario, since partons in the initial state cascade can have any kinematically allowed transverse momentum, in contrast to DGLAP. The CCFM [17–20] approach and its reformulation in the Linked Dipole Chain Model LDC [21, 22] attempt to cover both the DGLAP and BFKL regions by considering color coherence effects. A general introduction to small-x physics and the evolution equations can be found in [23].

2. CCFM–LDC evolution and unintegrated parton densities

In the CCFM evolution equation angular ordering of emissions is introduced to correctly treat gluon coherence effects. In the limit of asymptotic energies, it is almost equivalent to BFKL [24–26], but also similar to the DGLAP evolution for large x and high Q^2. The cross section is k_t-factorized into an off-shell matrix element convoluted with an unintegrated parton density (uPDF), which now also contains a dependence on the maximum angle Ξ allowed in emissions. This maximum allowed angle Ξ is defined by the hard scattering quark box, producing the (heavy) quark pair and also defines the scale for which parton emissions are factorized into the uPDF.

The original CCFM splitting function is given by:

$$P_g = \frac{\bar{\alpha}_s(p_t)}{1-z} + \frac{\bar{\alpha}_s(k_t)}{z}\Delta_{ns} \quad \text{with} \quad \log \Delta_{ns} = -\int\limits_{z_i}^{1} \frac{dz'}{z'} \int\limits_{(z'\bar{q}_i)^2}^{k_{ti}^2} \frac{dq^2}{q^2}\bar{\alpha}_s \qquad (1)$$

with $\bar{\alpha}_s = \frac{3\alpha_s}{\pi}$. The phase space region of angular ordered emissions is obtained from:

$$z_{i-1}\bar{q}_{i-1} < \bar{q}_i \quad \text{with} \quad \bar{q}_i = \frac{p_{ti}}{1-z_i}. \qquad (2)$$

Here $z_i = x_i/x_{i-1}$ is the ratio of the energy fractions in the branching $(i-1) \to i$ and p_{ti} is the transverse momentum of the emitted gluon i. The transverse momentum of the propagating gluon is given by k_{ti}. It is interesting to note, that the angular ordering constraint, as given by Eq. (2), reduces to ordering in transverse momenta p_t for large z, whereas for $z \to 0$, the transverse momenta are free to perform a so-called random walk.

The LDC model is a reformulation of CCFM, where the separation between the initial- and final-state emissions is redefined and, in addition to the angular ordering in Eq. (2), the gluons emitted in the initial state are required to have

$$p_{ti} > \min(k_{ti}, k_{ti-1}). \qquad (3)$$

This constraint means that the p_t of the emitted gluon is always close to the highest scale in the splitting and the argument in α_s is naturally taken to be p_t.

While formally equivalent to the DLLA accuracy, it is important to note that the sets of chains of initial-state splittings summed over, are different in LDC and CCFM. One chain in LDC corresponds to a whole set of chains in CCFM, and predictions for non-inclusive observables of the evolution will only be comparable if the correct final-state emissions are added in the regions relevant for the formalism used.

The CASCADE [27,28] program is a direct implementation of the CCFM approach into a hadron level Monte Carlo generator using a backward evolution approach for the initial state parton shower. The LDC [29,30] program is a realization of the LDC model in terms of a hadron level Monte Carlo generator.

2.1. Unintegrated gluon densities

The original CCFM splitting function given in Eq. (1) includes only the singular terms as well as a simplified treatment of the scale in α_s. Due to the angular ordering a kind of random walk in the propagator gluon k_t can be performed, and therefore care has to be taken for small values of k_t. For values of $k_t < k_t^{cut}$ the non-perturbative region is entered, which is avoided in a strictly p_t-ordered evolution (DGLAP). In CCFM, for $k_t < k_t^{cut}$, $\alpha_s(k_t)$ and also the splitting probability could become un-physically large. However, this is the region of high parton densities, where saturation effects could appear. A practical treatment here is to freeze α_s and the gluon density for values $k_t < k_t^{cut}$.

Three new sets of uPDFs were determined [31]:

J2003 set 1 with the splitting function given in Eq. (1),

J2003 set 2 including also the non-singular terms in P_g and

J2003 set 3 using p_t as the argument in α_s.

For all sets the input parameters were fitted to describe the structure function F_2 as measured at H1 [32, 33] and ZEUS [34, 35] in the range of $x < 10^{-2}$ and $Q^2 > 5\,\text{GeV}^2$. Using 248 data points a $\chi^2/\text{ndf} = 1.29, 1.18, 1.83$ for *J2003 set 1,2,3* , respectively, is obtained. A comparison of the different sets of CCFM uPDFs is shown in Fig. 1.

Also the LDC model describes F_2 satisfactorily well, but the corresponding unintegrated gluon densities are somewhat different, as also quarks can be included in the evolution. In Fig. 2 three different unintegrated gluon densities for the LDC approach are presented. The *standard* set refers to
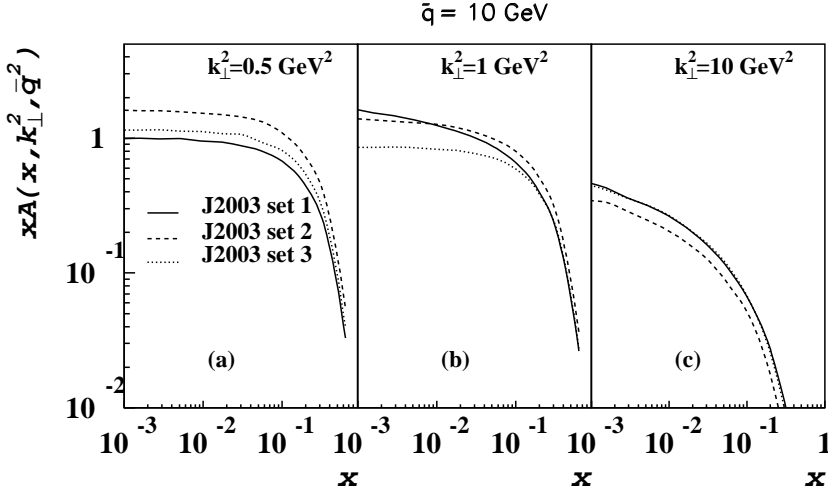
Fig. 1. Comparison of the different sets of unintegrated gluon densities obtained from the CCFM evolution as a function of x for different values of k_t at a scale of $\bar{q} = 10$ GeV.
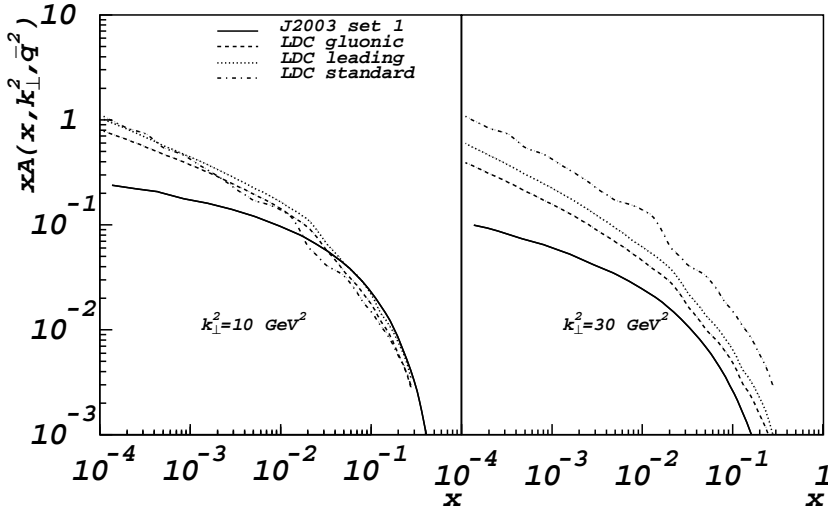

Fig. 2. Comparison of the different sets of unintegrated gluon densities obtained within LDC at scale of $\bar{q} = 10$ GeV. Standard refers to the full LDC including quarks in the evolution and the full gluon splitting function. For gluonic and leading only gluon evolution is considered with only singular terms in the splitting function for the latter. Also shown is the *J2003 set 1* for comparison (divided by π).

the full LDC including quarks in the evolution and the full gluon splitting function, whereas for the *gluonic* set and the *leading* set only gluon evolution is considered with only singular terms in the splitting function for the latter. All three alternatives have been individually fitted to F_2 in the region $x < 0.3$, $Q^2 > 1.5$ GeV^2 for *standard* and $x < 0.013$ and $Q^2 > 3.5$ GeV^2 for *gluonic* and *leading*. In LDC there is only one relevant infrared cutoff, k_{t0}, which limits the p_t of emitted gluons.

3. Comparison with hadronic final state data

A comparison of measurements of hadronic final state properties, like jet or heavy quark cross sections, with theoretical predictions requires Monte Carlo event generators, which also allow to apply the hadronization step. In the following sections a few examples are presented where data are compared to predictions obtained with CASCADE based on the CCFM unintegrated gluon densities, described in Section 2.1.

3.1. Jet cross section at HERA

The azimuthal correlation of dijets at HERA is sensitive to the transverse momentum of the partons incoming to the hard scattering process and therefore sensitive to the details of the unintegrated gluon density. This was studied in a measurement [36] of the cross section for dijet production with $E_T > 5(7)$ GeV in the range $1 < \eta_{lab} < 0.5$ in deep-inelastic scattering ($10^{-4} < x < 10^{-2}$, $5 < Q^2 < 100$ GeV^2). In LO collinear factorization, dijets at small x_{Bj} are produced essentially by $\gamma g \rightarrow q\bar{q}$, with the gluon collinear to the incoming proton. Therefore the $q\bar{q}$ pair is produced back-to-back in the plane transverse to the $\gamma^* p$ direction. From NLO ($\mathcal{O}(\alpha_s^2)$) on, significant deviations from the back-to-back scenario can be expected. In the k_t-factorization approach the transverse momentum of the incoming gluon, described by the unintegrated gluon density, is taken explicitly into account, resulting in deviations from a pure back-to-back configuration. The azimuthal de-correlation, as suggested in Ref. [37], can be measured:

$$S = \frac{\int_0^\alpha N_{2-\text{jet}}(\Delta\phi^*, x, Q^2) d\Delta\phi^*}{\int_0^{180^\circ} N_{2-\text{jet}}(\Delta\phi^*, x, Q^2) d\Delta\phi^*}, \quad 0 < \alpha < 180^\circ. \qquad (4)$$

In the measurement shown in Fig. 3, $\alpha = 120^\circ$ has been chosen. The data are compared to predictions from CASCADE using *J2003 set 1–3*. Also shown for comparison is the NLO-dijet [38] calculation of the collinear approach.

One clearly sees, that a fixed order NLO-dijet calculation is not sufficient, whereas *J2003 set 2* gives a good description of the data. However, the variable S is sensitive to the details of the unintegrated gluon distribution, as can be seen from the comparison with *J2003 set 1* and *set 3*.
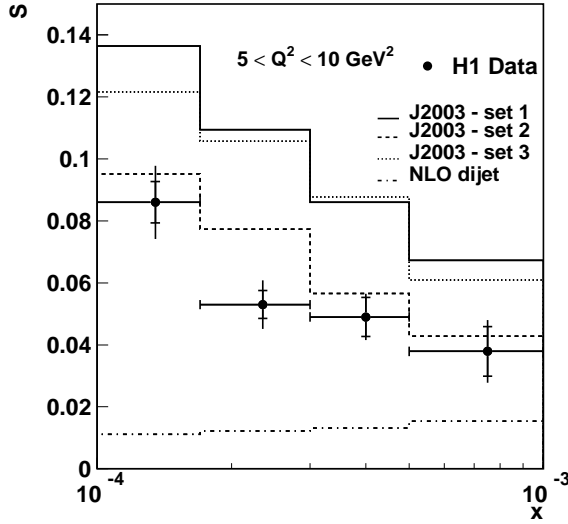

Fig. 3. The S distribution for dijet events [36]. The prediction from CASCADE are shown together with the NLO-dijet prediction in the collinear factorization approach.
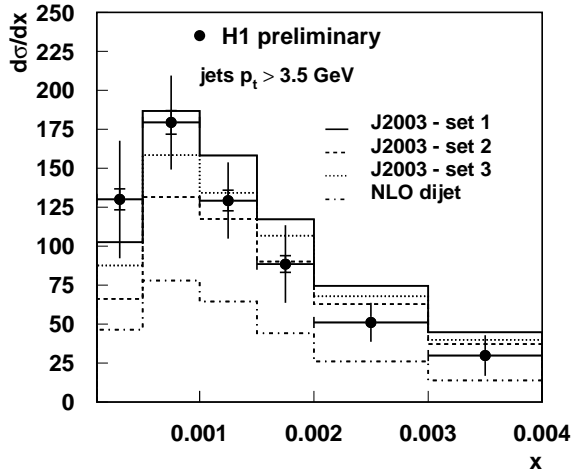

Fig. 4. The cross section for forward jet production as measured by H1 [39] as a function of x_{Bj}. The prediction are the same as in Fig. 3.

A measurement, aiming to observe deviations from the collinear DGLAP approach, is the production of jets in the forward (proton) region. The phase space is restricted to a region of $Q^2 > 5$ GeV^2 and $E_{\text{T}}^{\text{jet}} > 3.5$ GeV in the forward region of $1.7 < \eta_{\text{jet}} < 2.8$ with the additional requirement of $0.5 < E_{\text{T,jet}}^2/Q^2 < 2$, a region where the contribution from the evolution in Q^2 is small. The cross section for forward jet production has been measured by H1 [39] as a function of x_{Bj}, shown in Fig. 4 together with predictions from CASCADE. Also the NLO-dijet [38] prediction in the collinear approach is shown. The fixed NLO-dijet calculation falls below the measurement, whereas the k_{t}-factorization approach supplemented with CCFM evolution gives a reasonable description of the data.

3.2. Heavy quark production at the Tevatron

The differential cross section as a function of the transverse momentum of D-mesons has been measured in $p\bar{p}$ collisions at $\sqrt{s} = 1.96$ TeV by the CDF Collaboration [40]. They find the measured cross section to be larger than the NLO predictions in the collinear factorization approach by about 100 % at low p_{t} and 50 % at high p_{t}. In Fig. 5 the measurement is shown together with the predictions obtained in k_{t}-factorization using CASCADE with the CCFM unintegrated gluon density described above. For *J2003 set 1* and *set 3* good agreement for all measured charmed mesons is observed.
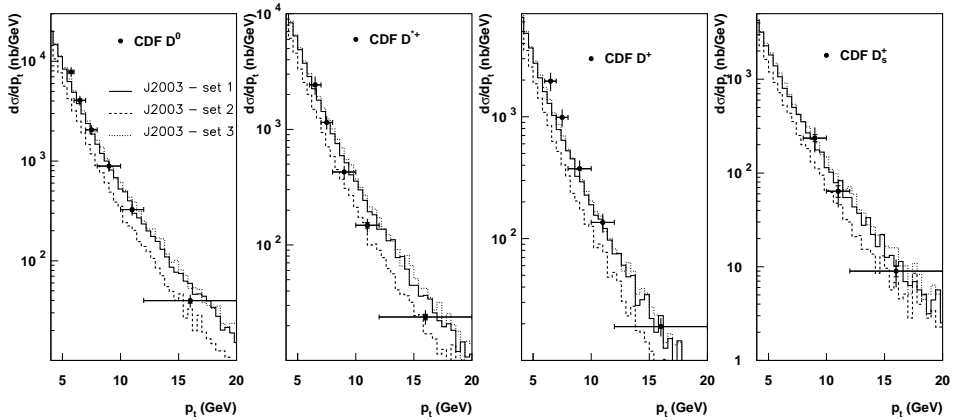

Fig. 5. Differential cross section for D meson production as measured by CDF [40] as a function of the transverse momentum compared to predictions from CASCADE.

The cross section for $b\bar{b}$ production in $p\bar{p}$ collision at $\sqrt{s} = 1800$ GeV has been compared with the prediction of CASCADE based on the CCFM gluon densities in [41]. It is interesting to note that *J2003 set 2* which describes best the data of Fig. 3, predicts a lower cross section for heavy quark production.

4. Conclusion

It has been shown, that k_t-factorization and the CCFM evolution of the gluon density is a powerful tool for the description of hadronic final state measurements. Improvements of the CCFM splitting function have been discussed.

Jet measurements at HERA, but also measurements of charm and bottom production at the Tevatron can be reasonably well described, whereas calculations performed in the collinear approach even in NLO have difficulties to describe the data. This shows the advantage of applying k_t-factorization to estimate higher order contributions to the cross section but also the importance of a detailed understanding of the parton evolution process.

It is a pleasure to thank A. Bialas, K. Fialkowski, K. Golec-Biernat, B. Brzezicka and the whole crew for this interesting and stimulating workshop.

REFERENCES

 [1] C. Adloff *et al.* (H1 Collaboration), `hep-ex/0304003`.
 [2] ZEUS Collaboration S. Chekanov *et al.*, *Phys. Rev.* **D67**, 012007 (2003).
 [3] C. Adloff *et al.* , *Eur. Phys. J.* **C19**, 289 (2001).
 [4] J. Breitweg *et al.* , *Phys. Lett.* **B507**, 70 (2001).
 [5] B. Abbott *et al.*, *Phys. Rev. Lett.* **82**, 2457 (1999).
 [6] V. Gribov, L. Lipatov, *Sov. J. Nucl. Phys.* **15**, 438 and 675 (1972).
 [7] L. Lipatov, *Sov. J. Nucl. Phys.* **20**, 94 (1975).
 [8] G. Altarelli, G. Parisi, *Nucl. Phys.* **B126**, 298 (1977).
 [9] Y. Dokshitser, *Sov. Phys. JETP* **46**, 641 (1977).
[10] E. Kuraev, L. Lipatov, V. Fadin, *Sov. Phys. JETP* **44**, 443 (1976).
[11] E. Kuraev, L. Lipatov, V. Fadin, *Sov. Phys. JETP* **45**, 199 (1977).
[12] Y. Balitskii, L. Lipatov, *Sov. J. Nucl. Phys.* **28**, 822 (1978).
[13] S. Catani, M. Ciafaloni, F. Hautmann, *Nucl. Phys.* **B366**, 135 (1991).
[14] J. Collins, R. Ellis, *Nucl. Phys.* **B360**, 3 (1991).

[15] L. Gribov, E. Levin, M. Ryskin, *Phys. Rep.* **100**, 1 (1983).

[16] E.M. Levin, M.G. Ryskin, Y.M. Shabelski, A.G. Shuvaev, *Sov. J. Nucl. Phys.* **53**, 657 (1991).

[17] M. Ciafaloni, *Nucl. Phys.* **B296**, 49 (1988).

[18] S. Catani, F. Fiorani, G. Marchesini, *Phys. Lett.* **B234**, 339 (1990).

[19] S. Catani, F. Fiorani, G. Marchesini, *Nucl. Phys.* **B336**, 18 (1990).

[20] G. Marchesini, *Nucl. Phys.* **B445**, 49 (1995).

[21] B. Andersson, G. Gustafson, J. Samuelsson, *Nucl. Phys.* **B467**, 443 (1996).

[22] B. Andersson, G. Gustafson, H. Kharraziha, J. Samuelsson, *Z. Phys.* **C71**, 613 (1996).

[23] B. Andersson *et al.* (Small x Collaboration), *Eur. Phys. J.* **C25**, 77 (2002).

[24] J.R. Forshaw, A. Sabio Vera, *Phys. Lett.* **B440**, 141 (1998).

[25] B.R. Webber, *Phys. Lett.* **B444**, 81 (1998).

[26] G. Salam, *J. High Energy Phys.* **03**, 009 (1999).

[27] H. Jung, G. Salam, *Eur. Phys. J.* **C19**, 351 (2001).

[28] H. Jung, *Comput. Phys. Commun.* **143**, 100 (2002), `http://www.quark.lu.se/ hannes/cascade/`.

[29] G. Gustafson, H. Kharraziha, L. Lönnblad, *Proc. of the Workshop on Future Physics at HERA*, eds. A. De Roeck, G. Ingelman, R. Klanner, 1996, p. 620.

[30] H. Kharraziha, L. Lönnblad, *J. High Energy Phys.* **03**, 006 (1998).

[31] M. Hansson, H. Jung, `hep-ph/0309009`.

[32] (H1 Collaboration) S. Aid *et al.* , *Nucl. Phys.* **B470**, 3 (1996).

[33] H1 Collaboration, C. Adloff *et al.* , *Eur. Phys. J.* **C21**, 33 (2001).

[34] ZEUS Collaboration; M. Derrick *et al.*, *Z. Phys.* **C72**, 399 (1996).

[35] (ZEUS Collaboration) S. Chekanov *et al.*, *Eur. Phys. J.* **C21**, 443 (2001).

[36] (H1 Collaboration) A. Aktas *et al.*, `hep-ex/0310019`.

[37] A. Szczurek, N.N. Nikolaev, W. Schafer, J. Speth, *Phys. Lett.* **B500**, 254 (2001).

[38] S. Catani, M.H. Seymour, *Nucl. Phys.* **B485**, 291 (1997).

[39] H. Jung, for H1 and ZEUS Collaborations, *Nucl. Phys. B - Proc. Suppl.* **117**, 352 (2002).

[40] CDF Collaboration D. Acosta *et al.*, `hep-ex/0307080`.

[41] H. Jung, `hep-ph/0311249`, to be published in *Mod. Phys. Lett.* **A**.